LAWRENCE
LIVERMORE
NATIONAL
LABORATORY

UCRL-PROC-204146

Intracavity adaptive correction of a 10 kW, solid-state, heat-capacity laser

K. N. LaFortune, R. L. Hurd, J. M. Brase, R. M. Yamamoto

May 13, 2004

Solid State & Diode Laser Technology Review
Albuquerque, NM, United States
June 8, 2004 through June 10, 2004

Intracavity adaptive correction of a 10 kW, solid-state, heat-capacity laser

K. N. LaFortune, R. L. Hurd, J. M. Brase, R. M. Yamamoto

University of California
Lawrence Livermore National Laboratory
Livermore, CA 94551

The Solid-State, Heat-Capacity Laser (SSHCL), under development at Lawrence Livermore National Laboratory (LLNL) is a large aperture (100 cm^2), confocal, unstable resonator requiring near-diffraction-limited beam quality. There are two primary sources of the aberrations in the system: residual, static aberrations from the fabrication of the optical components and predictable, time-dependent, thermally-induced index gradients within the gain medium. A deformable mirror placed within the cavity is used to correct the aberrations that are sensed externally with a Shack-Hartmann wavefront sensor. Although the complexity of intracavity adaptive correction is greater than that of external correction, it enables control of the mode growth within the resonator, resulting in the ability to correct a more aberrated system longer. The overall system design, measurement techniques and correction algorithms are discussed. Experimental results from initial correction of the static aberrations and dynamic correction of the time-dependent aberrations are presented.

For many applications, the optical quality of laser's output is a driving factor in its design. Often chosen for their propagation characteristics, lasers can perform more poorly than incoherent sources if there is no consideration given to wavefront quality. The primary cause of wavefront degradation in many lasers is thermally-induced index gradients. Lasers can be designed to minimize the impact of these thermal aberrations.[1] But, in the design of high-energy lasers, it is not always possible to design out all of the thermal aberrations. In this case, additional measures must be taken. One approach is the use of an adaptive optics control system similar to those used in astronomy.[2] Wavefront control of lasers using adaptive optics is nothing new. Typically, though, extra-cavity correction is employed because implementation is much easier than intracavity correction. However, intracavity correction provides additional benefits such as control over mode growth. Implementing an adaptive optics control system inside a resonator can difficult for many reasons. The primary reason is that there is not a one-to-one correspondence between the phase that can be measured and the phase that needs to be applied as a correction. Fortunately, the relationship between an intracavity corrector and the phase sensor has been well developed for an unstable resonator.[3] It can be approximated by a geometrical model. Previous experimental attempts at intracavity correction of a laser's output with adaptive optics resulted in limited success.[4–6] The SSHCL at LLNL is the first demonstration of a high-order, high-average-power, intracavity correction of an unstable resonator.

To zeroth order, the wavefront control of the LLNL system is achieved through the heat-capacity nature of the laser operation. The term "heat-capacity" refers to the fact that there is no active cooling of the laser during operation.[7] Heat that is deposited into the system, stays there. The heat-capacity of the components, in particular the gain medium, is used to store the heat for the duration of the laser operation. After a period of operation, the laser must be allowed to cool down. Although heat-capacity operation necessitates a pulsed or burst operation of the laser, it has the distinct advantage of greatly reduced aberrations over an actively cooled system. Because there is no active cooling, thermal gradients are minimized. This reduces the associated mechanical stresses. Temperature and stress dependent refractive index gradients are minimized. Deformation of the laser slabs, which also induces aberrations, is minimized. These shot-induced aberrations are still the largest component of the overall aberrations. But, they are very predictable. They depend upon the amount and distribution of heat deposited into the gain medium for each shot. This is determined by the geometry of the system and is fixed.

There are two other components of aberrations. The first is thermal diffusion of the energy deposited in the gain medium. This is the least predictable because it depends upon the laser's history: how many shots have been fired recently and when. Fortunately, its effects cannot be seen during operation because its time

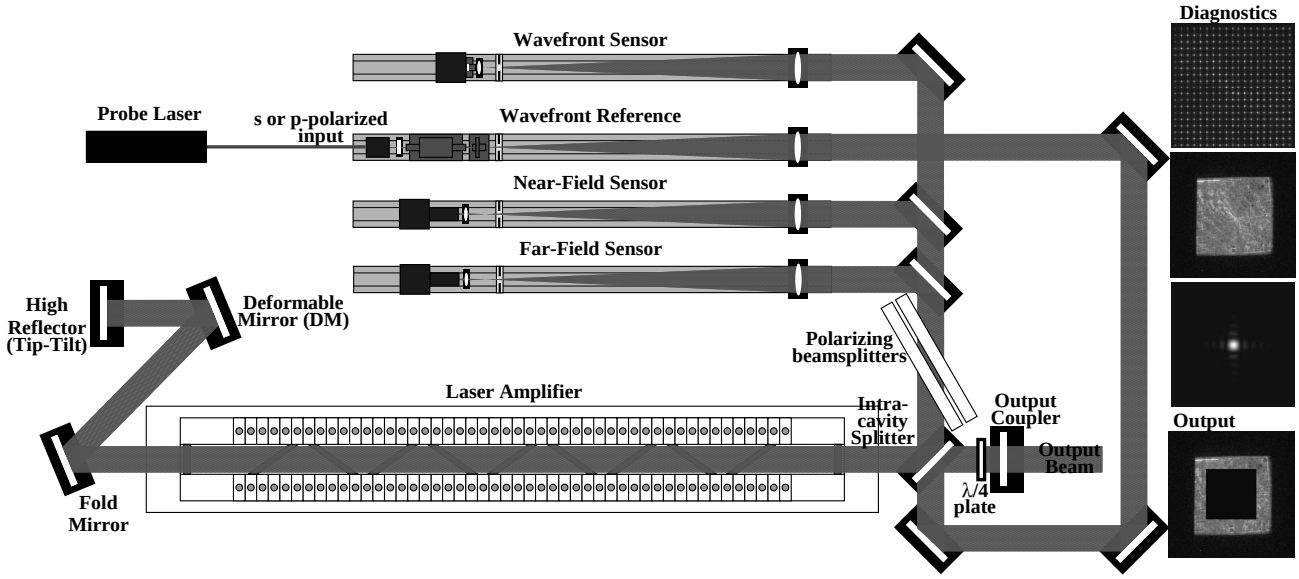

Figure 1. The system layout of the adaptively-corrected, unstable resonator. Shown are the three diagnostic paths and representative images of their output: Shack-Hartmann wavefront sensor, near-field and far-field cameras. Polarization selection is used to probe the cavity. The deformable mirror and tip-tilt correction are both at one end of the cavity. The amplifier contains nine flashlamp-pumped Nd:glass slabs at Brewster's angle. The output of the laser is a square annulus.

constant is too long. The second is the static aberrations induced by fabrication and alignment errors in the optics. These only change when components are replaced. Thermal diffusion and static aberrations are easily compensated for either in the first few pulses of operation or before operation with the probe laser because they are slowly changing. The shot-induced aberrations are more difficult to compensate for because they are larger and more rapidly changing. Fortunately, their repeatability lends them to predictive correction, which can compensate for the majority of their growth.

All of these phase errors contribute to a degradation in laser performance. Not only is the output wavefront aberrated, but the magnitude of the aberrations can be large enough to induce intensity modulation across the aperture. A problem for which extra-cavity correction does not provide a solution. Intracavity correction can provide a solution but involves a nonintuitive relationship between the output phase of the laser and the correction that must be applied to make that phase flat. The relationship is, in fact, nonlinear and analytically solvable in only a few cases. Fortunately, it can be approximated by a linear theory in the limit in which the aberrations are small.

The intracavity, adaptive-optic resonator (Figure 1), is built into the second-generation, solid-state, heat-capacity laser at LLNL. This laser is capable of producing 10 kW of average power at 1053 nm. It is a pulsed laser, running at up to 20 Hz for a burst of up to 200 shots. After each burst, the laser is allowed to cool. Each pulse is 500 μsec long. The clear aperture is a square 10 cm on a side. The geometry is a positive-branch, confocal, unstable resonator with a magnification of 1.5. The output profile of a laser with such a geometry is a square annulus with inner dimensions of 6 2/3 cm on a side.

The wavefront must be measured and controlled over the whole 10 cm by 10 cm area. Therefore a beam splitter is used within the cavity to couple the full beam profile to the diagnostics. In addition to far-field and near-field diagnostics, there is a Shack-Hartmann wavefront sensor (WFS), which is used to measure the gradient of the phase on a 19 by 19 grid. The average phase within each sampling interval is measured. The sensor was designed for a sensitivity exceeding $\lambda/10$.

The deformable mirror (DM) is designed to work with the WFS to compensate for the measured aberrations. Manufactured by Xinetics Corp., it has a ULE face-sheet, supported by 206 PMN actuators on a pseudo-

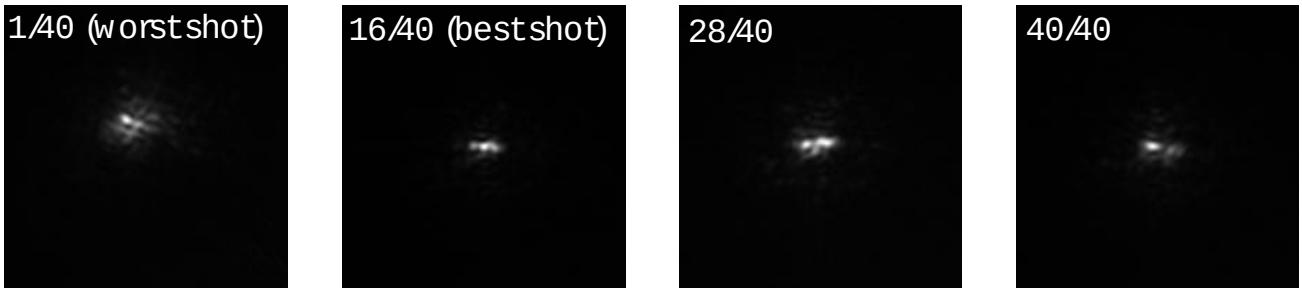

Figure 2. Far-field images of selected pulses showing the laser performance during a 40 pulse run. The best pulse (as measured by a power-in-a-bucket analysis) is shown.

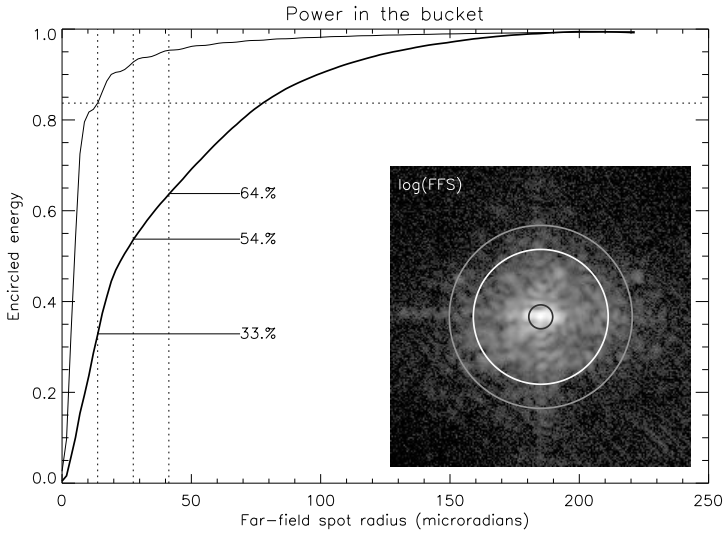

Figure 3. Power-in-a-bucket plot of the best (16 th) pulse from the sequence in Figure 2. The diffraction limited spot size is the radius to the first minimum. Vertical dotted lines are drawn at the 1x, 2x and 3x diffraction-limited radii. The fraction of the total energy contained within each of these radii is shown. A logarithmic plot of the far-field diffraction pattern is shown. Superimposed are circles depicting the diffraction limited area (smallest), the (5.5) times-diffraction limited (xDL) area (middle) and the spatial frequency domain of the DM (largest). The horizontal scale is the divergence angle assuming 1 μm light propagating from a 10 cm aperture.

hexagonal grid with a nominal 1 cm actuator spacing. It was designed with a dynamic range of 10 μm, larger than the maximum observed aberration occurring in the system during its designed run time . There are 126 actuators within the clear aperture of the laser. It was manufactured to a tolerance of less than $\lambda/50$ RMS powered figure. It has a high-damage-threshold, high-reflectivity, multilayer-dielectric coating.

The primary metric for performance was the quality of a far-field spot. It should be noted that the far-field diagnostic, like the WFS, is sampled from the cavity before the beam has passed through the output-coupler. It is derived from the intensity profile of a fully-filled square aperture whereas the propagated beam is a square annulus. The divergence angle for the annular beam is about 3.2 times larger than that for the fully-filled case.

The metric by which the far-field performance is measured is somewhat a matter of preference. There are many metrics to choose from, some more appropriate than others depending on the nature of the beam to be characterized. Residual wavefront error is an option but not a very good one because it does not tell you anything about the energy distribution at the target. It is more appropriate to quantify the energy distribution of the diffraction pattern rather than the phase distribution in the near-field. If the propagating beam is Gaussian, M^2 may me the appropriate choice. A Strehl ratio is useful if the operating regime is one in which

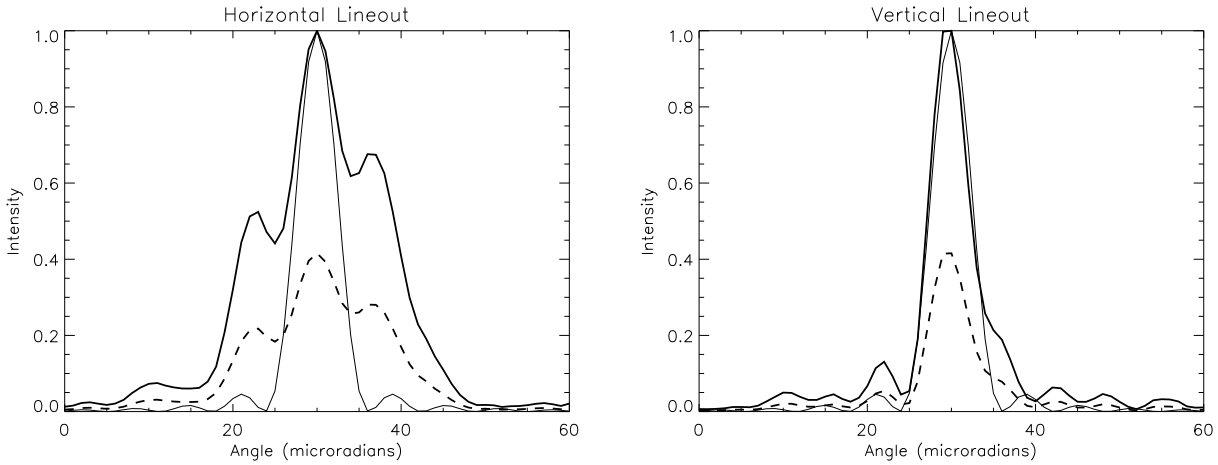

Figure 4. Horizontal and vertical line-outs of the best (16 th) pulse from the sequence in Figure 2. The peak-normalized intensity curve (thick, solid) and energy-normalized curve (thick-dashed) are compared to the theoretical limit (thin, solid). The energy-normalized curve reveals the Strehl ratio. The horizontal scale is the divergence angle assuming 1 μm light propagating from a 10 cm aperture.

the feature size or the propagation distance is large enough that only the central lobe of the far-field diffraction pattern will be used. The ratio of the actual spot radius to the theoretical limit, or "times-diffraction-limit" (xDL) number is more generally useful but is somewhat arbitrary. Different conventions are used to determine the radius. Although the temptation to reduce the wavefront quality to one number is great, a more descriptive metric is the encircled-energy, or power-in-a-bucket (PIB), curve. It is a plot of the fraction of energy contained within a radius as a function of the radius. It is, by definition, zero at a radius of zero and one at a radius of infinity. In between, one can find the xDL size (using any desired convention). The fraction of energy deposited within any desired divergence angle can be obtained. The Strehl ratio can also be estimated from the figure as the fraction of the energy within a 1xDL radius. A power-in-a-bucket curve for one of the pulses in the 40 shot run presented above appears in Figure 3. Line-outs of the same pulse appear in Figure 4. To perform a reliable PIB measurement, a 12 bit camera with low read noise (< 2 counts) and a large area (six times the area shown) needed to be used. Careless background subtraction or lower bit-depth resulted in artificially low xDL values.

Supported by U.S. Army Space and Missile Defense Command. This work was performed under the auspices of the U.S. Department of Energy by University of California, Lawrence Livermore National Laboratory under Contract W-7405-Eng-48. UCRL number: UCRL-PROC-201816

REFERENCES

1. J. Vetrovec, "Solid-state high-energy laser," *Proc. SPIE* **4632**, pp. 104–14, 2002.
2. C. E. Max, D. T. Gavel, and S. S. Olivier, "Near infra-red astronomy with adaptive optics and laser guide stars at the keck observatory," *Proc. SPIE* **2534**, pp. 412–22, 1995.
3. K. E. Oughstun, "Aberration sensitivity of unstable-cavity geometries," *J. Opt. Soc. Am. A - Optics & Image Science* **3**, pp. 1113–41, Aug. 1986.
4. J. M. Spinhirne, D. Analfi, R. H. Freeman, and H. R. Garcia, "Intracavity adaptive optics. i. astigmatism correction performance," *App. Opt.* **20**, p. 976, 1981.
5. D. Analfi, J. M. Spinhirne, R. H. Freeman, H. R. Garcia, and K. E. Oughstun, "Intracavity adaptive optics. ii. tilt correction performance," *App. Opt.* **20**, p. 1926, 1981.
6. K. E. Oughstun, J. M. Spinhirne, and D. Anafi, "Intracavity adaptive optics. iv. comparison of theory and experiment," *Appl. Opt.* **23**, pp. 1529–41, May 1984.
7. G. F. Albrecht, S. B. Sutton, E. V. George, W. R. Sooy, and W. F. Krupke, "Solid state heat capacity disk laser," *Laser and Particle Beams* **16**(4), p. 605, 1998.